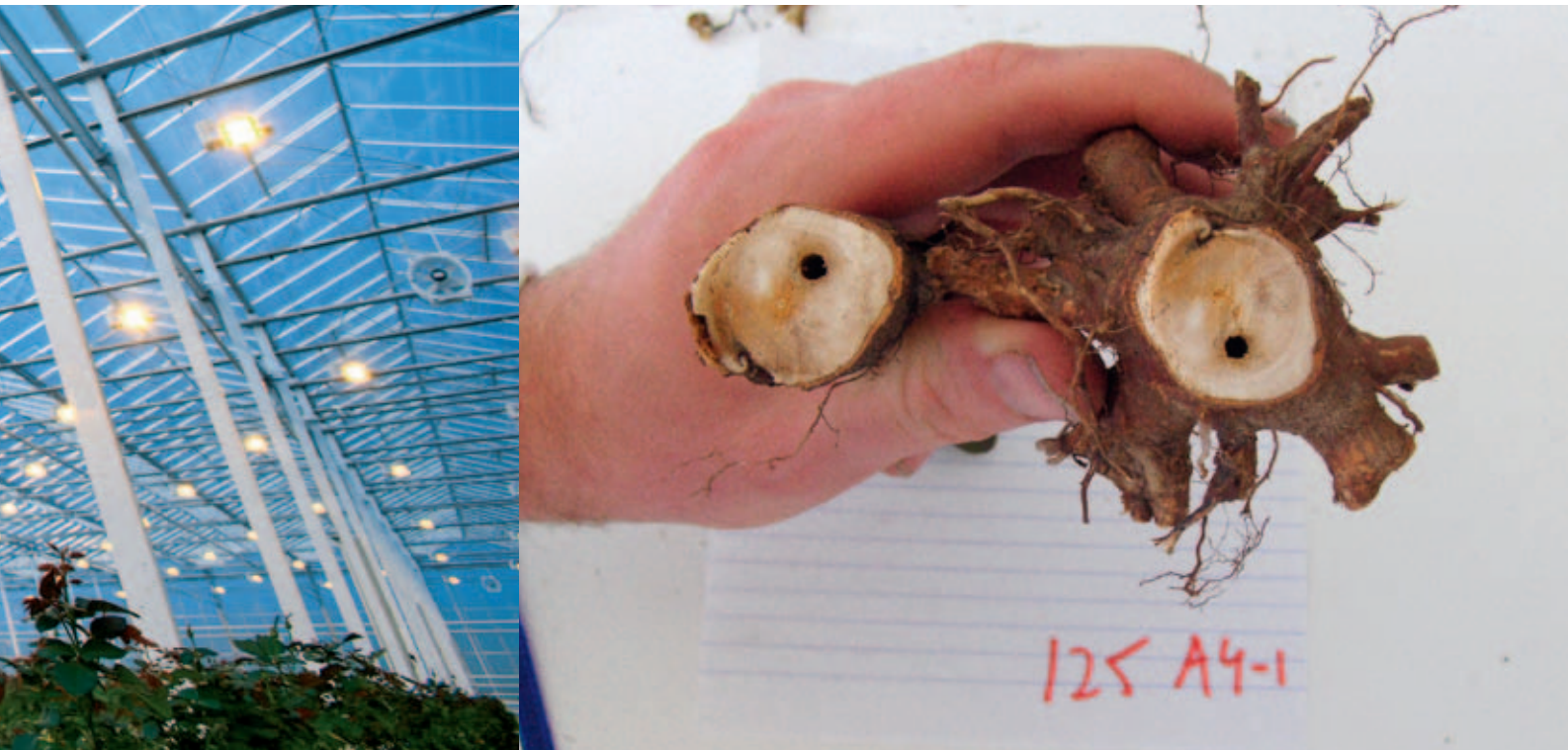




# Validation of X-ray for borehole detection in intact trees

R.M.C. Jansen, J. Hemming



Vertrouwelijk rapport GTB-5026

© 2011 Wageningen, Wageningen UR Greenhouse Horticulture (Wageningen UR Glastuinbouw).

## **Wageningen UR Greenhouse Horticulture**

Adres : Droevedaalsesteeg 1, 6708 PB Wageningen, the Netherlands  
: P.O. Box 16, 6700 AA Wageningen, the Netherlands  
Tel. : +31 317 - 48 60 01  
Fax : +31 317 - 41 80 94  
E-mail : [greenhousehorticulture@wur.nl](mailto:greenhousehorticulture@wur.nl)  
Internet : [www.greenhousehorticulture.wur.nl](http://www.greenhousehorticulture.wur.nl)

# Table of contents

	Summary	5
	Acknowledgement	7
1	Introduction	9
2	Materials and methods	11
2.1	X-ray inspection system	11
2.2	Optimisation of the borehole detection method	11
2.3	Validation of the optimised borehole detection method	11
2.4	Combining machine vision and human input	12
3	Results	13
3.1	Optimisation of the borehole detection method	13
3.2	Validation of the optimised borehole detection method	16
3.3	Combining machine vision and human input	21
4	Discussion	25
5	Conclusions and future directions	27
6	References	29
Appendix A	Results of manual scoring	31



## **Summary**

There is an increasing threat of harmful impact in EU territory arising from the increase of material infested by the Citrus long-horned beetles (*Anoplophora chinensis*). After import, wood material originating from infested areas should be monitored for the presence of any life stage of the long-horned beetle including egg, larva and pupa. Early detection would allow implementation of measures to reduce the incidence of beetle introduction. X-ray provides an important contribution to current research related to early and non-invasive detection of long beetle boreholes. Our previous research showed that X-ray-based machine vision can be used to automatically detect long-horned beetle induced boreholes in intact trees by. Yet, a large number of unaffected trees was incorrectly classified as borehole affected.

The first objective of the present research was to improve the previous borehole detection method and to validate the performance of tree classification using an improved machine vision algorithm using morphological operators. The second objective of the present research was to test whether the borehole detection could be further improved by combining machine vision and human input. To test the effect of combining machine vision and human input, a user friendly application was developed. This application consisted of the optimised borehole detection algorithm integrated into a graphical user interface, which was used to show the X-ray images to two observers one after the other. In case the borehole detection algorithm detected a borehole, a red line was blinking at the expected borehole position. Optimisation of the borehole detection algorithm resulted in an increase in the accuracy of the method from 3% to 67% while the sensitivity remained at 83%. Combining machine vision and human input resulted in a further increase in accuracy up to 83%. The developed method is therefore useful for future usage in early detection of long-horned beetles.

The present research was based on X-ray images recorded on a system dedicated to luggage inspection. We suggest to design and build an X-ray instrument dedicated to phytosanitary inspection in the future. Next to that the effect of operator training should be studied. Research on the detection of other phytosanitary problems using X-ray is highly recommended. This research was financed by the Dutch Food Safety Authority (nVWA) and was carried out under assistance of Dutch General Inspection Service (NAK Tuinbouw), the Dutch Customs Laboratory and Siemens



## **Acknowledgement**

The authors acknowledge Henk Lemmen, Ad Sonnemans and Ron Bleijswijk from the Dutch General Inspection Service (NAK Tuinbouw) and Nico Mentink, Brigitta Wessels and Barend Mechelsen from the new Dutch Food Safety Authority (nVWA) for their assistance during the research. Furthermore we acknowledge Antoon Loomans and Paul van den Boogert for their support. We also acknowledge the management of the Dutch Customs Laboratory and thank Siemens for installation of the X-ray system. Finally, we acknowledge the nVWA for financial assistance.



# 1 Introduction

There is an increasing threat of harmful impact in EU territory arising from the increase of material infested by the Citrus long-horned beetle (*Anoplophora chinensis*). The Citrus long-horned beetle is native to China and other nearby Pacific Rim countries (Moraal and Wessels-Berk, 2007). They were probably introduced into the EU through import of wood material from one of these countries (Moraal and Wessels-Berk, 2007). After import, wood material originating from infested areas should be monitored for the presence of any life stage of the long-horned beetle including egg, larva and pupa. Early detection would allow implementation of measures to reduce the incidence of beetle introduction. Besides the presence of life stages of the Citrus long-horned beetle, other symptoms may indicate long-horned beetle infestation. One such symptom is the presence of boreholes.

X-ray provides an important contribution to current research related to early and non-invasive detection of boreholes. Work on this line was carried out by Fischer & Tasker (1945), Cruvinel *et al.* (2003) and Tomazello *et al.* (2008) who all used X-ray photographs to inspect wood pieces for the presence of insect infestation. During 2009-2010, we did preliminary tests to study whether X-ray can be used to detect boreholes. Results demonstrated that artificial boreholes and long-horned beetle induced boreholes were detectable in wood pieces (de Kogel *et al.* 2010) and in intact trees (Jansen and Hemming, 2010). For intact trees, a computer vision method was developed to automate the detection of boreholes (Jansen and Hemming, 2010). Using this method, digital images from a total of 929 Japanese maple trees was analysed for the presence of boreholes. This approach resulted in the automated detection of boreholes in intact trees (Jansen and Hemming, 2010). Besides the correct classification of trees as borehole affected, a large number of trees were incorrectly classified as borehole affected. This inaccuracy was mainly the result of gaps in-between roots and branches which were incorrectly identified as boreholes (Figure 1.).

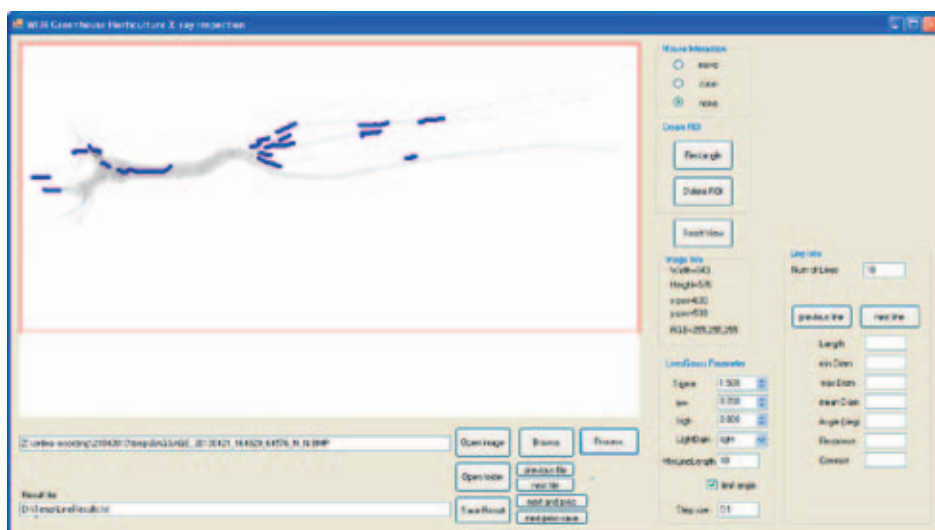


Figure 1. Automated detection of a borehole in the stem of an intact Japanese maple tree. Besides the borehole, also gaps in-between roots and branches were incorrectly identified as boreholes.

The first objective of the present research was to improve the existing borehole detection method and to validate the performance of tree classification using the improved method. The research question was: what is the effect of improving the borehole detection method on the performance of tree classification?

It was expected that the performance of tree classification would further improve by combining machine vision and human input. For instance, in the first step the machine vision gives a warning in case a tree is classified as suspicious. In the second step, the observer investigates the image to see whether it indeed contains signs of borehole presence. The second objective of the present research was to test whether the borehole detection method could be further improved by combining machine vision and human input. The associated research questions was: what is the effect of combining machine vision and human input on the performance of tree classification?



## 2 Materials and methods

### 2.1 X-ray inspection system

X-ray images were recorded on a luggage X-ray inspection system (Hi-Scan 6040i; Smiths Heimann, Germany). Such systems are commonly used on airports for inspection of luggage. The X-ray tube —source of the electromagnetic radiation— was located on the right side of the system underneath the conveyor. The conveyor speed was approximately 0.2 m/s. The tunnel dimensions are 620 mm (W) x 418 mm (H). The anode voltage of the X-ray generator was approximately 140 kV.

### 2.2 Optimisation of the borehole detection method

Halcon v. 10.0 was used for optimising *version 1* of the borehole detection method described in (Jansen & Hemming 2010). The optimisation was achieved by focusing the region of interest (ROI) to the main trunk and the root part only and by deleting the small structures before further processing.

The following image processing steps are carried out:

1. Fixed thresholding of input grey value x-ray image to segment object(s) of interests from background
2. Applying morphological operators to locate the main stem in the image
  - a. Erosion by circular mask.
  - b. Connected components labelling.
  - c. Selection of biggest remaining object.
  - d. Dilation by same circular mask.
3. Intersection of dilated regions with binary image. The object with the largest number of pixels represents now the main trunk of the tree.
4. As the main orientation of the object in the image is known a priori and boreholes are expected at the root end and not at the crown end of the tree the ROI is decreased by removing the crown part of the tree from the ROI.
5. As in version 1 at this point a lines gauss detection was performed to this ROI. For details is referred to Jansen & Hemming (2010).

The dataset for optimisation consisted of 929 X-ray images.

### 2.3 Validation of the optimised borehole detection method

The dataset for validation consisted of 1204 X-ray images not used for optimisation. Classification of this dataset by the optimised borehole detection method resulted in a number of:

- True positives (TP); in this case, one or more boreholes are detected. After destructive assessment it was confirmed that the tree contains one or more boreholes.
- True negatives (TN); in this case, no borehole is detected. After destructive assessment it was confirmed that the tree does not contain any borehole.
- False positives (FP); in this case, one or more boreholes are detected. After destructive assessment, it turns out that the tree does not contain any borehole.
- False negatives (FN); in this case, no borehole is detected. After destructive assessment, it turns out that the tree contains one or more boreholes.

In the present research, the term 'accuracy' is used to test the performance of tree classification:

$$\text{accuracy} = \frac{\text{number of true positives} + \text{number of true negatives}}{\text{number of true positives} + \text{false positives} + \text{false negatives} + \text{true negatives}} \quad \text{Equation 1}$$

Furthermore, we use the term 'sensitivity' to test the ability to identify positive results.

$$\text{sensitivity} = \frac{\text{number of true positives}}{\text{number of true positives} + \text{false negatives}} \quad \text{Equation 2}$$

## 2.4 Combining machine vision and human input

A user friendly application was developed to test the effect of combining machine vision and human input on the performance of tree classification. This application consisted of the optimised borehole detection method integrated into a graphical user interface (GUI). Using this GUI, the X-ray images are shown to an observer one after the other. The maximum time period per image is adjustable. In case the borehole detection method detects a borehole, a red line is blinking at the expected borehole position. Based on the judgement of the observer and results from the destructive assessment (Jansen & Hemming 2010), we calculated the number of true positives, true negatives, false positives and false negatives. These numbers are then stored in a data-file which can be opened in MS-Excel.

The effect of combining machine vision and human input was studied using two observers working for the NAK Tuinbouw (The Dutch General Inspection Service) and thus experienced in tree observation. A collection of one hundred X-ray images were shown to these observers. This collection consisted of 18 X-ray images of trees which were classified as suspicious after destructive assessment and 82 randomly selected X-ray images of trees which were classified as unsuspicious after destructive assessment. In the present research, the maximum time period per image was set at 10 sec.

Before starting the experiment, the two observers were trained for 30 min. During training, the GUI was used to show these observers twenty X-ray images of pre-drilled stems containing artificial boreholes with a length of 30-50 mm and a diameter of  $\varnothing=3, 4, \text{ or } 5 \text{ mm}$ . A screenshot of the GUI containing an X-ray image of a stem containing an artificial boreholes of  $\varnothing=4 \text{ mm}$  is provided in Figure 2.

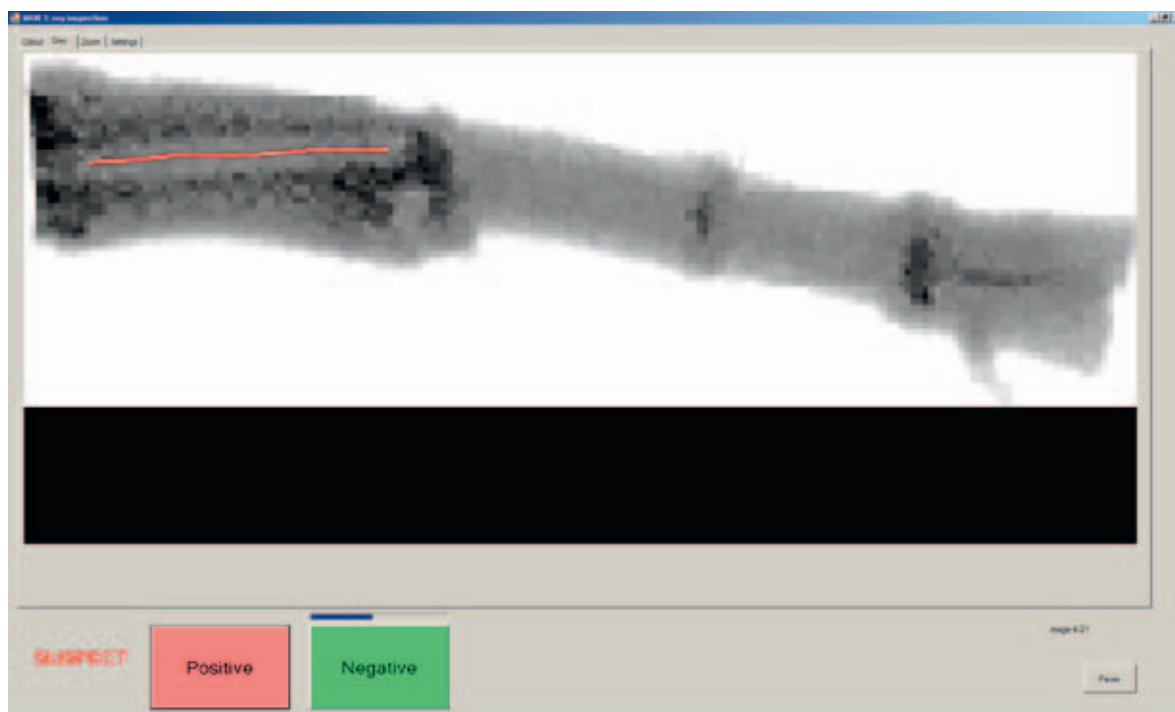


Figure 2. Screenshot containing an X-ray image of a stem containing an artificial borehole of  $\varnothing=4 \text{ mm}$ . These type of images were shown to the two observers during training.

### 3 Results

#### 3.1 Optimisation of the borehole detection method

The dataset for optimisation consisted of 929 X-ray images. The number of true positives, true negatives, false positives, and false negatives after optimisation of the borehole detection method are presented in Table 1.

*Table 1. Number of true positives, true negatives, false positives, and false negatives as a result of the optimised borehole detection method.*

Classification	Version 1	Optimised version
True positives	5	5
True negatives	26	625
False positives	899	300
False negatives	1	1
TOTAL	929	929

As can be seen from Table 1, the optimisation resulted in a 24-fold increase in the number of true negatives and a 3-fold reduce in the number of false positives. The numbers of true positives and false negatives remained equal (Table 1.). Based on these numbers and Eq. 1, the accuracy of the method increased from 3% to 67%. Based on these numbers and Eq. 2, the sensitivity of the method remained 83%.

Figure 3. provides the effect of optimisation for a tree in which no borehole was found after destructive assessment. Such a tree was classified as false positive in version 1 of the borehole detection method but correctly classified as true negative in the optimised version of the borehole detection method.

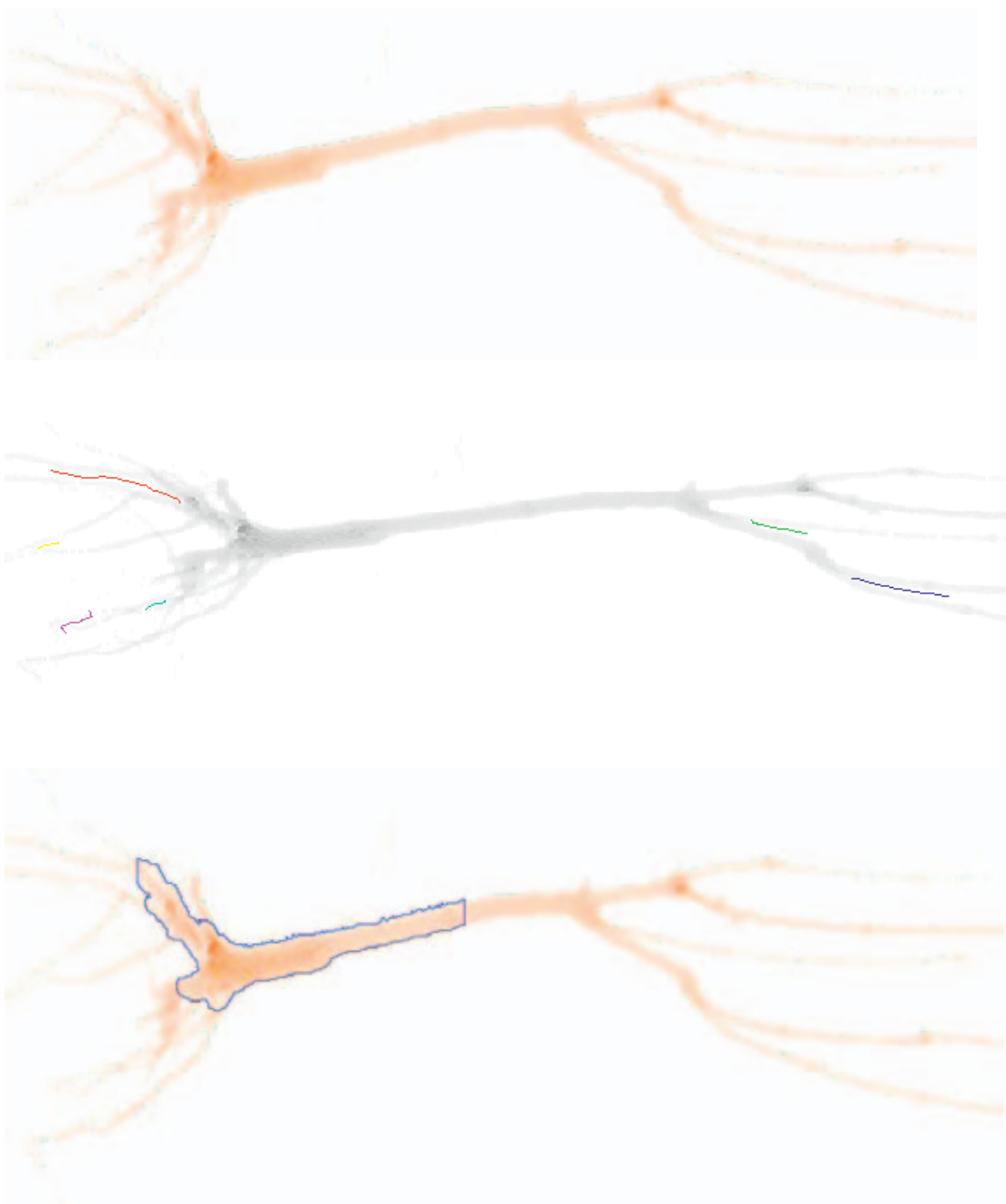


Figure 3. The effect of optimisation of the borehole detection method for a true negative. Top Original X-ray image; Middle borehole detection before optimisation; Bottom borehole detection after optimisation of the borehole detection method.

Figure 4. provides the effect of optimisation for a tree in which a borehole was found after destructive assessment.

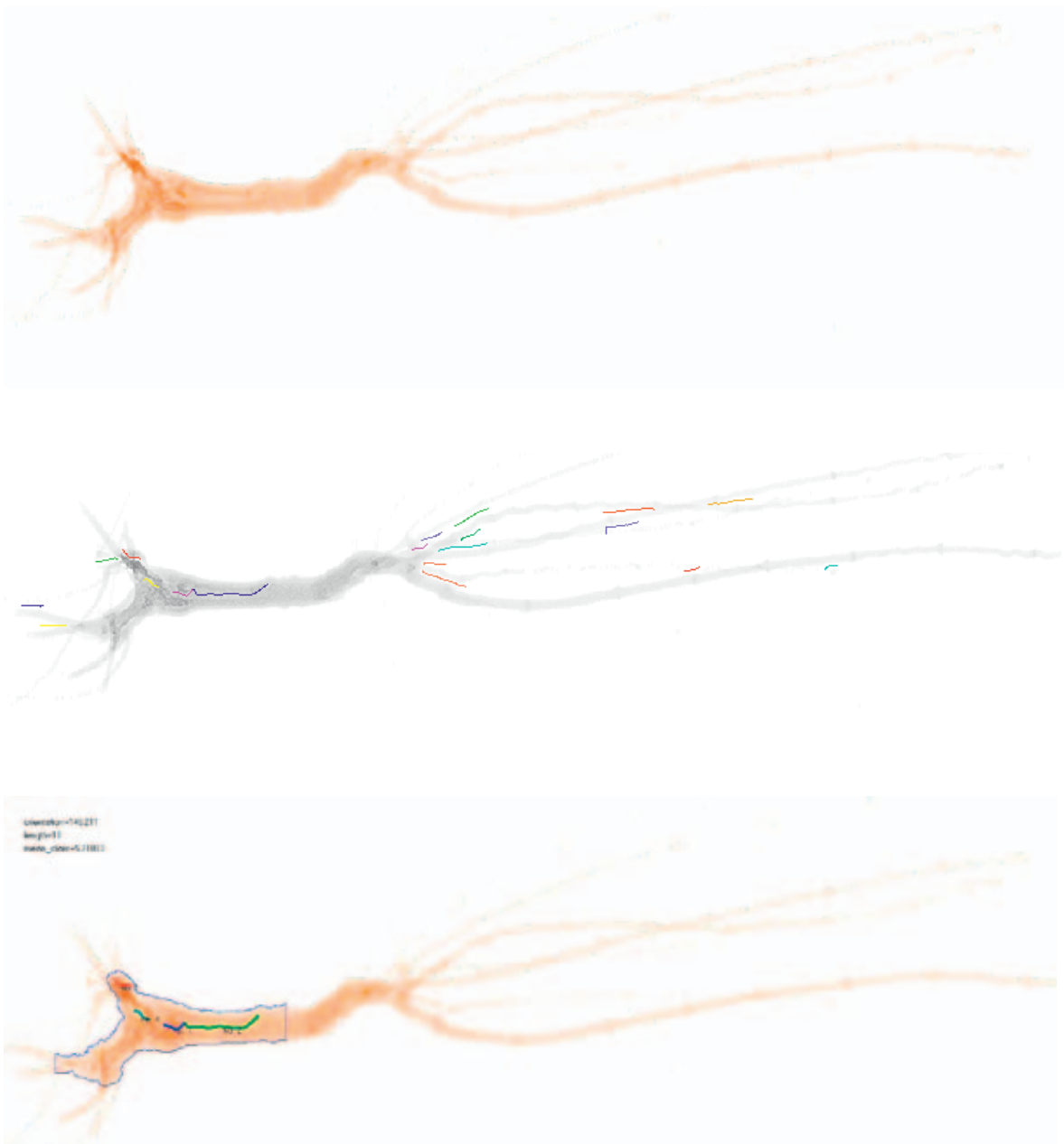


Figure 4. The effect of optimisation the borehole detection method for a true positive. Top Original X-ray image; Middle borehole detection before optimisation; Bottom borehole detection after optimisation of the borehole detection method.

## 3.2 Validation of the optimised borehole detection method

A dataset consisting of 1204 X-ray images was used to validate the optimised borehole detection method. Table 2. presents the number of true positives, true negatives, false positives, and false negatives after validation of the optimised borehole detection method. According to Eq. 1 and Eq. 2, these numbers resulted in an accuracy of 72% and a sensitivity of 56%.

*Table 2. Number of true positives, true negatives, false positives, and false negatives after validation of the optimised borehole detection method.*

Classification	Nr.
True positives	10
True negatives	851
False positives	335
False negatives	8
TOTAL	1204

Examples of a true positive, a true negative, a false positive and a false negative are provided in respectively Figure 5., Figure 6., Figure 7., and Figure 8.



Figure 5. Example of a true positive in the validation dataset. Top original X-ray image; Bottom borehole detection after validation of the borehole detection method.

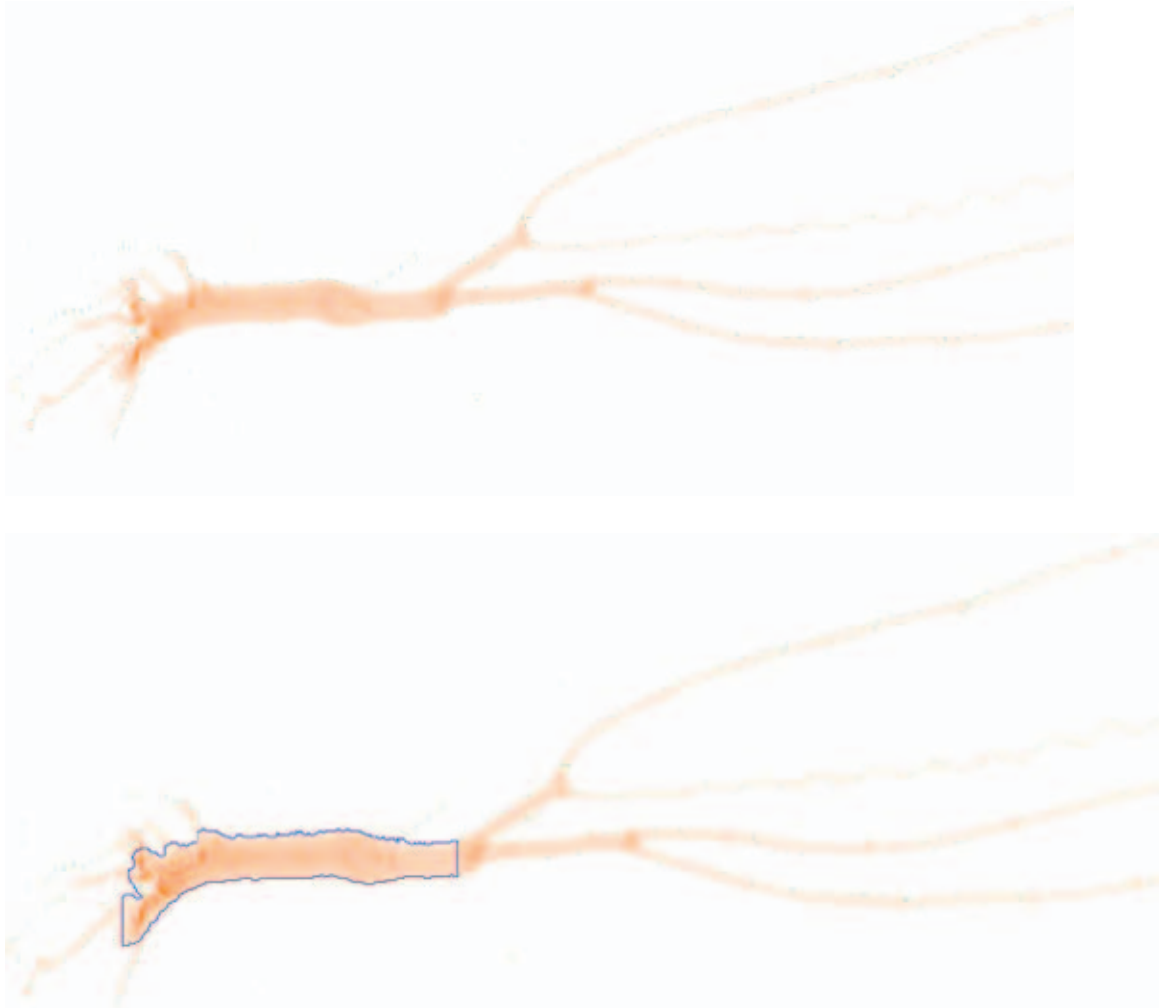


Figure 6. Example of a true negative in the validation dataset. Top original X-ray image; Bottom borehole detection after validation of the borehole detection method.



Figure 7. Example of a false positive in the validation dataset. Top original X-ray image; Bottom borehole detection after validation of the borehole detection method.



*Figure 8. Example of a false negative in the validation dataset. Top original X-ray image; Bottom borehole detection after validation of the borehole detection method.*

### 3.3 Combining machine vision and human input

One hundred X-ray images were shown to two observers to test whether the borehole detection could be further improved by combining machine vision and human input. Table 3. presents the number of true positives, true negatives, false positives, and false negatives when using machine vision and when using the combination of machine vision and human input. Details regarding the machine vision and the manual score are provided in Appendix A.

*Table 3. Number of true positives, true negatives, false positives, and false negatives for machine vision and for the combination machine vision and human input. Results are provided for two observers.*

Classification	Machine vision	Machine vision + observer 1	Machine vision + observer 2
True positives	9	9	9
True negatives	49	72	74
False positives	33	10	8
False negatives	9	9	9
TOTAL	100	100	100

The accuracy (Eq. 1) and sensitivity (Eq. 2) for machine vision and the combination of machine vision and human input are provided in Table 4.

*Table 4. Accuracy and sensitivity for machine vision and the combination of machine vision and human input.*

Measure	Machine vision	Machine vision + observer 1	Machine vision + observer 2
Accuracy	61%	82%	83%
Sensitivity	56%	50%	50%

From Table 3., it can be seen that the total number of true positives remains equal when combining machine vision and human input. Nevertheless, X-ray images of suspicious trees (true positives) were classified dissimilar. For instance, two X-ray images of suspicious trees were classified as negative by machine vision but classified as positive by both observers (Figure 9.). Also the opposite occurred: two X-ray images of suspicious trees (true positives) were classified as positive by machine vision but classified as negative by both observers (Figure 10.). The classification of the observers was similar: 88% of the images were classified equal.

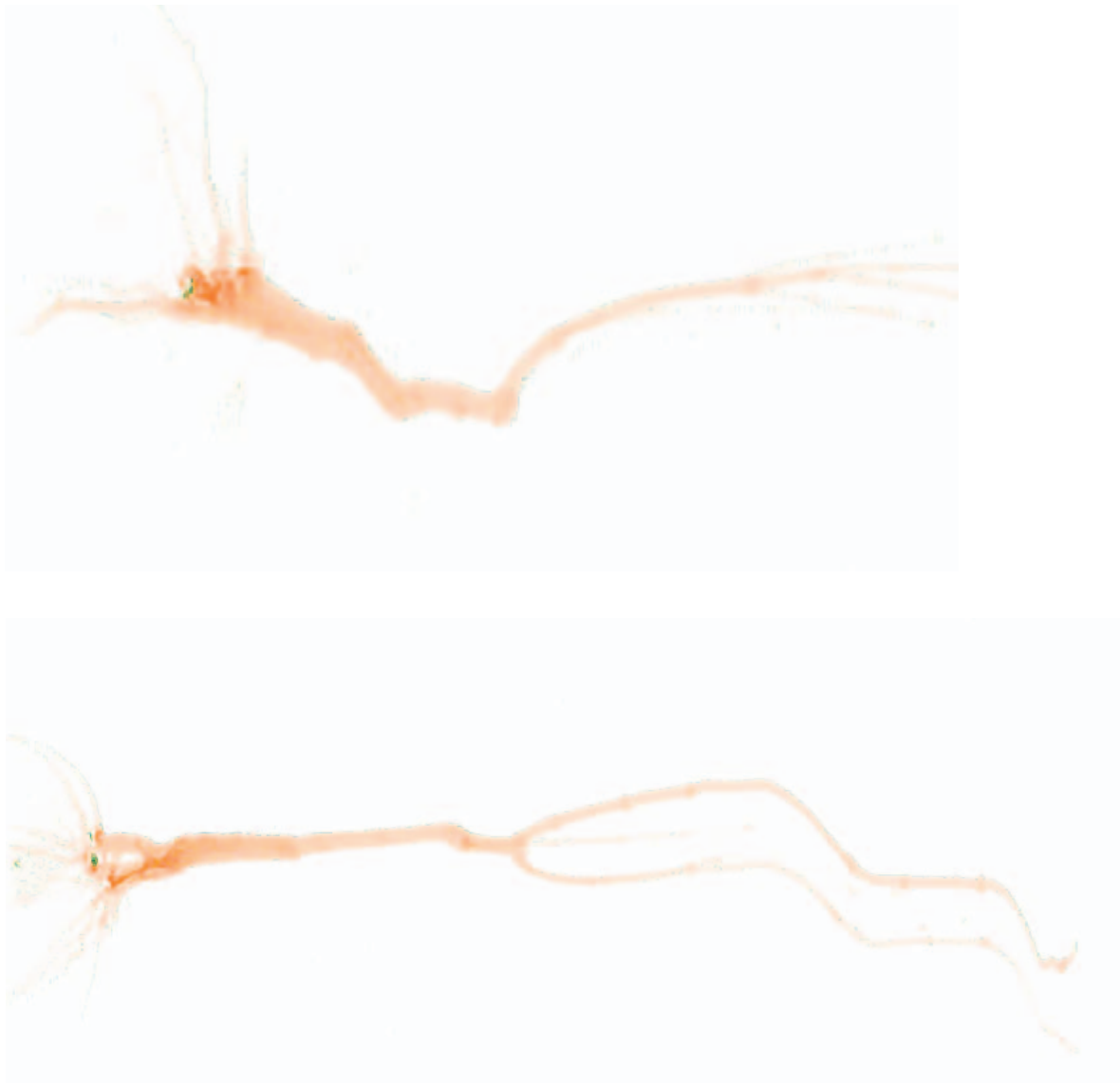


*Figure 9. X-ray images of two suspicious trees (true positives) which were classified as negative by machine vision but classified as positives by both observers. The reason for negative classification of the top image by machine vision is the constraint applied the boreholes has to be orientated nearly parallel to the centre line of the main stem (the angle was limited to +45° till -45°).*



*Figure 10. X-ray images of two suspicious trees (true positives) which were classified as positives by machine vision but classified as negatives by both observers.*



## 4 Discussion

The first objective of the present research was to improve the existing borehole detection method and to validate the performance of tree classification using the improved method. Results demonstrate that the accuracy of the improved method increased from 3% to 67% while the sensitivity of the method remained 83%. This increase was due to improved machine vision method. We expect that the accuracy and sensitivity would further increase when using a better-quality instrument. For instance, both the accuracy and the sensitivity would further increases in case higher resolution images are produced. A higher resolution is feasible: the resolutions of an X-ray instruments dedicated to phytosanitary inspection is 0.5–0.6 mm (Chuang *et al.* 2011), while the resolution of the X-ray images used in this study is about 1 mm. Also other instrument related parameters such as the current and the voltage were not optimised for borehole detection. We thus suggest to fine-tune existing X-ray instruments and to redesign and build an X-ray instrument specifically dedicated to phytosanitary inspection of agricultural products including seeds, fruits, trees and plants. Depending on requirements and available budget, this instrument could be transportable such as some of the X-ray scanning systems in use by the Dutch Customs Laboratory (Figure 11.). Also portable X-ray scanning systems have been developed (Kim *et al.* 2011).



Figure 11. Transportable X-ray instrument currently in use by the Dutch Customs Laboratory.

The second objective of the present research was to test whether the borehole detection method could be further improved by combining machine vision and human input. Results demonstrate that the accuracy increased from 60% to 80% while the sensitivity remained similar. It is still unclear what the effect of training would be on this result. Therefore, it is suggested to also study the intra-observer variability and redo the experiment with certain time interval.

The present study demonstrated the suitability of X-ray for detection of boreholes caused by *Anoplophora chinensis*. This result agrees with other studies who showed the detection of fruit flies in several types of fruits including tomato, berry, orange, apple, pear and peach (Yang *et al.* 2006). Likely, X-ray instruments can be used more cost effective in case these phytosanitary problems are indeed detectable using X-ray. But, one could also think about other phytosanitary issues including problems in unions, carrots and fruits such as apples, pears or oranges. Therefore, we suggest to study whether other phytosanitary problems are also detectable using X-ray.

Few figures exist regarding costs and benefits of phytosanitary inspections: (1) per year, about 3.4 billion pieces of nursery stock are imported into The Netherlands; (2) the economic value of this type of material is about €4.5 billion; (3) per year, about 40.000 phytosanitary inspections are carried out (source: nVWA). These numbers provide some information about the relevance of inspection. Still, the costs and benefits of X-ray assisted inspection are largely unknown. Simulation models with the capability to vary inspection machine configuration and placement can be used to predict the economics of X-ray inspection technology (Mosqueda *et al.* 2010).

In this study, X-ray images were recorded on a 2-D scanner used for luggage inspection. Today, more advanced 3-D scanners are available: often referred to as X-ray computed tomography (CT).

A basic exploration of this method —also commissioned by the Plant Protection Service (nVWA)— has been performed for the detection of boreholes in wood (Mol and Wolf, 2011). These type of scanners are mainly used for medical imaging. Applying such instruments for phytosanitary inspection would definitely result in an increased accuracy and sensitivity. Therefore, we suggest to facilitate the exchange of knowledge between experts in the field of 3-D medical imaging and experts in the field of phytosanitary inspection.

## 5 Conclusions and future directions

Based on the results we conclude:

1. The combination of machine vision and human input results in an improved performance of X-ray assisted borehole detection for intact trees. We expect that training of X-ray operators will further improve this performance. However, the effect of operator training on the performance is mostly unknown. Therefore, we suggest to study the effect of operator training in order to quantify this effect.
2. To further improve the performance of X-ray based borehole detection, we suggest to design and build an X-ray instrument dedicated to phytosanitary inspection. When setting up a list of prerequisites for such an instrument, different stakeholders should participate. Stakeholders should include personnel working at NAK Tuinbouw, nVWA, and the Dutch Customs Laboratory. Also experts in phytosanitation should be included.
3. Besides long-horn induced boreholes in trees, many other phytosanitary problems exist. Therefore we suggest to study whether other phytosanitary problems are also detectable using X-ray. One could think about phytosanitary problems with onions, carrots, apples, pears.
4. The costs and benefits of X-ray assisted inspection is largely unknown. We suggest to study these costs and benefits in detail in order to determine the profitability of X-ray assisted inspection. Do not only consider direct costs but also indirect costs such as reputation damage.
5. Probably, the future direction in X-ray inspection is 3-D imaging. Enabling the exchange of knowledge and instruments between companies that produce 3-D imaging instruments for the medical sectors and experts in the field of phytosanitation is therefore required.



## 6 References

- Chuang, C. L., C. S. Ouyang, et al. (2011)  
"Automatic x-ray quarantine scanner and pest infestation detector for agricultural products." Computers and Electronics in Agriculture 77(1): 41-59.
- Cruvinel, P.E., Naime, J.d.M., Borges, M., Macedo, A., Zhang, A. (2003)  
Detection of beetle damage in forests by x-ray CT image processing. Rivista Arvore, 27(5), 747-752.
- de Kogel, W.J., Helsper, H., Jalink, H., Jansen, R.M.C., Wiegers, G., van Deventer, P. (2010)  
Bruikbaarheid van non-destructive detectietechnologieën voor routinematige inspecties, Wageningen.
- Fischer, R.C. and Tasker, H.S. (1945)  
The detection of wood-boring insects by means of X-rays. Annals of Applied Biology, 27(1), 92-100.
- Jansen, R.M.C. and Hemming, J. (2010)  
X-ray inspection for boreholes in intact trees, Wageningen UR Greenhouse Horticulture, Wageningen.
- Kim, K.H., Kwak, S.W., Jung, Y.H. (2011)  
Development of a portable X-ray scan system (PXSS). Nuclear Instruments and Methods in Physical Research Section A, 648, S224-S227.
- Mol, C. and Wolf, R.M. (2011)  
3D Imaging for the detection of Anophlophora in wood, Philips Research, Eindhoven: pp 30.
- Moraal, L. and Wessels-Berk, B. (2007)  
Aziatische boktor dreigend gevaar. In Tuin&Landschap: pp 32-33.
- Mosqueda, M.R.P., Tollner, E.W., Boyhan, G.E., McClendon, R.W. (2010)  
Predicting the economics of X-ray inspection technology in sweet onion packinghouses using simulation modelling. Biosystems Engineering, 105(1), 139-147.
- Tomazelllo, M., Brazolin, S., Chagas, M.P., Oliveira, J.T.S., Ballarin, A.W. (2008)  
Application of X-Ray technique in nondestructive evaluation of euralypt wood. Ciencia y tecnologia, 10(2), 139-149.
- Yang, E.C., Yang, M.M., Liao, L.H., Wu, W.Y. (2006)  
Non-destructive quarantine technique- potential application of Using X-ray iamges to detect early infestation caused by oriental fruit fly (*Bactrocera dorsalis*) (Diptera: Tephritidae) in Fruit. Formosan Entomology, 26, 171-186.



# Appendix A Results of manual scoring

session started=8-9-2011 10:28:54 0:\Boktor\Human_Input (101 files)							
Bank				Ad			
file	time	result	timeout	time	result	timeout	visionscore
BAGGAGE_20100416_132329_64576_N_N_BMF	44,100,062	0	0	24,000,034	0	0	0
BAGGAGE_20100416_132526_64576_N_N_BMF	27,800,039	0	0	23,600,033	0	0	0
BAGGAGE_20100416_132739_64576_N_N_BMF	2,890,004	0	0	31,300,043	0	0	0
BAGGAGE_20100416_133011_64576_N_N_BMF	39,200,042	0	0	34,000,047	0	0	1
BAGGAGE_20100416_133154_64576_N_N_BMF	34,000,047	0	0	45,000,063	0	0	0
BAGGAGE_20100416_133466_64576_N_N_BMF	26,400,037	0	0	44,900,063	0	0	0
BAGGAGE_20100416_133602_64576_N_N_BMF	25,600,036	0	0	52,500,073	0	0	0
BAGGAGE_20100416_133832_64576_N_N_BMF	61,400,086	0	0	40,400,057	0	0	0
BAGGAGE_20100416_134054_64576_N_N_BMF	57,800,081	0	0	36,500,051	0	0	1
BAGGAGE_20100416_134329_64576_N_N_BMF	14,600,021	0	0	45,500,064	0	0	1
BAGGAGE_20100416_134958_64576_N_N_BMF	37,500,052	0	0	3,630,005	0	0	1
BAGGAGE_20100416_140021_64576_N_N_BMF	10,000,014	1	1	46,300,065	0	0	1
BAGGAGE_20100416_140155_64576_N_N_BMF	0,2300003	0	0	61,000,085	0	0	0
BAGGAGE_20100416_140334_64576_N_N_BMF	30,200,042	0	0	37,600,053	0	0	1
BAGGAGE_20100416_152808_64576_N_N_BMF	26,800,058	0	0	2,850,004	0	0	1
BAGGAGE_20100416_153144_64576_N_N_BMF	38,300,054	0	0	61,600,087	0	0	0
BAGGAGE_20100416_154544_64576_N_N_BMF	54,500,077	0	0	46,100,064	0	0	0
BAGGAGE_20100420_101969_64576_N_N_BMF	68,000,096	1	0	74,600,104	0	0	0
BAGGAGE_20100420_102658_64576_N_N_BMF	36,600,051	0	0	55,300,077	0	0	0
BAGGAGE_20100420_108119_64576_N_N_BMF	4,580,007	0	0	83,100,112	0	0	0
BAGGAGE_20100420_108224_64576_N_N_BMF	50,200,071	0	0	77,700,109	0	0	0
BAGGAGE_20100420_115735_64576_N_N_BMF	43,900,061	0	0	38,600,054	0	0	0
BAGGAGE_20100420_115900_64576_N_N_BMF	46,100,064	0	0	58,000,082	0	0	0
BAGGAGE_20100420_115928_64576_N_N_BMF	5,050,007	0	0	91,100,127	1	0	1
BAGGAGE_20100420_120087_64576_N_N_BMF	59,300,083	1	0	12,800,018	0	0	1
BAGGAGE_20100420_120315_64576_N_N_BMF	711,001	0	0	6,430,009	0	0	0
BAGGAGE_20100420_120414_64576_N_N_BMF	56,800,079	0	0	40,400,057	0	0	1
BAGGAGE_20100420_120436_64576_N_N_BMF	37,900,054	0	0	9,950,014	1	0	1
BAGGAGE_20100420_120531_64576_N_N_BMF	42,000,059	0	0	2,900,004	0	0	0
BAGGAGE_20100420_121008_64576_N_N_BMF	47,700,067	0	0	719,001	0	0	0
BAGGAGE_20100420_121026_64576_N_N_BMF	44,300,062	0	0	83,400,117	0	0	0
BAGGAGE_20100420_121121_64576_N_N_BMF	56,600,079	1	0	98,000,137	0	0	1
BAGGAGE_20100420_122204_64576_N_N_BMF	84,800,118	1	0	17,200,024	1	0	1
BAGGAGE_20100420_130309_64576_N_N_BMF	13,000,018	1	0	72,700,102	1	0	1
BAGGAGE_20100420_130321_64576_N_N_BMF	18,200,026	1	0	11,200,016	1	0	1
BAGGAGE_20100420_130323_64576_N_N_BMF	53,600,075	0	0	57,200,081	0	0	0
BAGGAGE_20100421_090102_64576_N_N_BMF	99,200,056	0	0	58,200,081	0	0	0
BAGGAGE_20100421_090714_64576_N_N_BMF	51,400,072	0	0	7,840,011	0	0	0
BAGGAGE_20100421_091003_64576_N_N_BMF	40,300,056	0	0	55,300,077	0	0	1
BAGGAGE_20100421_091410_64576_N_N_BMF	61,800,087	0	0	72,000,101	0	0	1
BAGGAGE_20100421_092254_64576_N_N_BMF	67,000,094	0	0	74,700,104	0	0	0
BAGGAGE_20100421_094125_64576_N_N_BMF	39,400,056	0	0	80,300,113	0	0	0
BAGGAGE_20100421_100810_64576_N_N_BMF	57,700,081	0	0	74,100,103	0	0	0
BAGGAGE_20100421_160131_64576_N_N_BMF	39,100,055	1	0	43,500,061	1	0	1
BAGGAGE_20100421_160216_64576_N_N_BMF	65,700,092	0	0	40,500,057	0	0	0
BAGGAGE_20100421_160315_64576_N_N_BMF	75,600,106	0	0	45,200,063	0	0	1
BAGGAGE_20100421_161049_64576_N_N_BMF	54,200,077	0	0	8,570,012	0	0	0
BAGGAGE_20100421_161100_64576_N_N_BMF	26,900,038	1	0	45,300,064	0	0	1
BAGGAGE_20100421_162209_64576_N_N_BMF	64,900,091	1	0	76,300,107	1	0	1
BAGGAGE_20100421_162249_64576_N_N_BMF	54,100,075	0	0	26,000,036	0	0	0
BAGGAGE_20100421_162802_64576_N_N_BMF	39,100,054	0	0	91,200,128	0	0	0
BAGGAGE_20100421_164407_64576_N_N_BMF	40,400,056	0	0	10,000,014	1	1	0
BAGGAGE_20100421_164714_64576_N_N_BMF	44,800,063	0	0	60,100,084	0	0	0
BAGGAGE_20100422_161029_64576_N_N_BMF	25,500,035	1	0	34,700,049	1	0	1
BAGGAGE_20100422_160934_64576_N_N_BMF	61,400,086	0	0	51,700,073	0	0	1
BAGGAGE_20100422_090208_64576_N_N_BMF	47,100,066	0	0	55,100,077	0	0	0
BAGGAGE_20100422_092700_64576_N_N_BMF	41,000,057	0	0	74,600,104	0	0	0
BAGGAGE_20100422_101002_64576_N_N_BMF	17,400,025	1	0	12,500,017	1	0	1
BAGGAGE_20100422_092507_64576_N_N_BMF	30,200,042	0	0	26,800,037	0	0	1
BAGGAGE_20100422_093100_64576_N_N_BMF	3,570,005	0	0	81,100,118	0	0	0
BAGGAGE_20100422_100913_64576_N_N_BMF	27,100,058	0	0	40,400,057	0	0	1
BAGGAGE_20100422_101235_64576_N_N_BMF	67,300,094	1	0	74,300,104	1	0	0
BAGGAGE_20100422_101347_64576_N_N_BMF	30,500,043	0	0	55,200,077	0	0	0
BAGGAGE_20100422_111311_64576_N_N_BMF	34,800,049	0	0	73,100,102	0	0	0
BAGGAGE_20100422_111531_64576_N_N_BMF	76,100,106	0	0	97,800,137	0	0	1
BAGGAGE_20100422_113026_64576_N_N_BMF	51,700,072	1	0	79,500,111	0	0	1
BAGGAGE_20100422_123920_64576_N_N_BMF	4,250,006	0	0	16,600,023	0	0	1
BAGGAGE_20100422_142421_64576_N_N_BMF	44,300,062	0	0	96,900,136	0	0	1
BAGGAGE_20100422_147852_64576_N_N_BMF	60,600,085	0	0	96,600,135	1	0	0
BAGGAGE_20100422_144529_64576_N_N_BMF	55,500,078	0	0	47,500,067	0	0	0
BAGGAGE_20100422_160211_64576_N_N_BMF	20,200,029	0	0	79,700,111	0	0	0
BAGGAGE_20100422_160254_64576_N_N_BMF	46,600,066	0	0	55,700,078	0	0	0
BAGGAGE_20100422_161012_64576_N_N_BMF	45,300,063	0	0	86,500,121	0	0	1
BAGGAGE_20100422_161032_64576_N_N_BMF	68,500,096	0	0	76,100,106	0	0	1
BAGGAGE_20100422_164537_64576_N_N_BMF	49,000,069	0	0	73,100,102	0	0	0
BAGGAGE_20100422_165116_64576_N_N_BMF	79,800,112	0	0	77,100,108	0	0	1
BAGGAGE_20100422_165117_64576_N_N_BMF	52,300,074	0	0	90,200,126	0	0	1
BAGGAGE_20100426_091903_64576_N_N_BMF	50,300,071	0	0	67,100,094	0	0	1
BAGGAGE_20100426_105135_64576_N_N_BMF	36,800,052	0	0	88,600,124	0	0	1
BAGGAGE_20100426_111905_64576_N_N_BMF	63,600,089	0	0	91,800,129	1	0	0

BAGGAGE_20100426_112915_64576_N_N.BMF	48,400,068	0	0	60,800,085	0	0	0	0	0	0	1
BAGGAGE_20100426_113949_64576_N_N.BMF	58,100,082	0	0	65,200,091	0	0	1	0	0	0	1
BAGGAGE_20100426_114121_64576_N_N.BMF	50,300,071	0	0	72,600,107	0	0	0	0	0	0	1
BAGGAGE_20100426_115214_64576_N_N.BMF	27,500,039	0	0	5,970,014	0	0	1	0	0	0	1
BAGGAGE_20100426_115220_64576_N_N.BMF	36,900,049	0	0	81,900,115	0	0	0	0	0	0	1
BAGGAGE_20100426_115413_64576_N_N.BMF	4,260,005	0	0	42,300,069	0	0	0	0	0	0	1
BAGGAGE_20100426_130927_64576_N_N.BMF	30,200,043	0	0	50,300,112	0	0	1	0	0	0	1
BAGGAGE_20100426_131018_64576_N_N.BMF	51,800,073	0	0	68,400,096	0	0	0	0	0	0	1
BAGGAGE_20100426_131032_64576_N_N.BMF	48,600,068	1	0	87,500,123	0	0	0	0	0	0	0
BAGGAGE_20100426_131039_64576_N_N.BMF	66,900,094	0	0	94,200,132	0	0	0	0	0	0	1
BAGGAGE_20100426_131128_64576_N_N.BMF	5,720,008	0	0	81,800,113	0	0	1	0	0	0	1
BAGGAGE_20100426_131140_64576_N_N.BMF	44,900,063	0	0	50,300,113	0	0	0	0	0	0	1
BAGGAGE_20100426_131238_64576_N_N.BMF	5,710,008	0	0	88,300,124	0	0	0	0	0	0	1
BAGGAGE_20100426_131241_64576_N_N.BMF	53,800,075	1	0	25,300,095	1	0	1	0	1	1	0
BAGGAGE_20100426_141045_64576_N_N.BMF	60,700,085	0	0	74,500,105	0	0	0	0	0	0	1
BAGGAGE_20100426_142713_64576_N_N.BMF	66,600,093	0	0	60,500,085	0	0	0	0	0	0	1
BAGGAGE_20100426_142817_64576_N_N.BMF	20,200,028	1	0	10,000,014	1	0	1	0	1	1	0
BAGGAGE_20100426_143024_64576_N_N.BMF	52,100,073	1	0	86,600,119	1	0	0	0	1	1	0
BAGGAGE_20100426_143037_64576_N_N.BMF	63,500,089	0	0	6,440,009	0	0	0	0	0	0	1
BAGGAGE_20100427_090259_64576_N_N.BMF	16,000,026	1	0	14,900,021	1	0	1	0	1	1	0
Total		19	1		17	1	42		18	12	76
									88		









Projectnummer: 3242108811